

## Optical spatial shock waves in photorefractive media

M. I. Carvalho

*Department of Electrical Engineering and Computers, Oporto University, Rua Dr. Roberto Frias, 4200-465, Porto, Portugal*

A. G. Grandpierre and D. N. Christodoulides

*Department of Electrical Engineering and Computer Science, Lehigh University, Bethlehem, Pennsylvania 18015*

M. Segev

*Physics Department, Technion-Israel Institute of Technology, Haifa 32000, Israel  
and Electrical Engineering Department, Princeton University, Princeton, New Jersey 08544*

(Received 13 April 2000)

We show that the evolution equations describing the two-wave mixing interaction between two codirectional optical beams in photorefractive media can allow spatial shock-wave solutions. Our analysis indicates that these kink-type wavefronts move together at an angle that falls outside the initial  $\pm\theta$  sector of propagation. The apparent direction of propagation and the spatial widths of these optical shock-wave beams are directly related to their relative intensity.

PACS number(s): 42.65.Tg, 42.65.Hw

### I. INTRODUCTION

Shock waves are ubiquitous entities that have been extensively investigated in several diverse areas of physics such as fluid mechanics, gas dynamics, plasma and solid-state physics [1,2]. Yet, in the field of optics, their occurrence is rather rare [3–12]. Thus far, in the optical domain, spatiotemporal shock (kink) waves have been identified in nonlinear systems with Raman nonlinearities [3–6], in dispersive amplifying nonlinear media that exhibit a frequency-dependent gain or loss [7,8], and in nonlinear media with higher-order nonlinearities [9,10]. It is clear from these previously mentioned examples that in many cases [3–8] such optical shock waves can occur provided that an energy exchange process is present during propagation. This process can be, for instance, stimulated Raman scattering between a Stokes and pump wave [4], intrapulse Raman scattering within a single shock-wave state [3,5,6] or a frequency-dependent amplification [7,8]. In view of the above discussion, it may be reasonable to ask whether spatial shock waves can also exist as a result of some energy exchange mechanism. This could be achieved for example via two-wave mixing that naturally occurs in photorefractives [13–21]. Aside from two-wave mixing, photorefractive crystals are known to host several other important nonlinear processes. These include four-wave mixing, phase conjugation [13–16], and spatial solitons [22–28]. Like shock waves, photorefractive spatial solitons retain their form during propagation. They owe their existence to the drift/photovoltaic component [25,26,28] of the photorefractive nonlinearity and can be observed at very low power levels. Bright and dark, one- and two-dimensional solitons have been systematically demonstrated in laboratory experiments. However, in contrast to shock waves, spatial photorefractive solitons rely on a conservative drift/photovoltaic nonlinearity (i.e., no power exchange takes place during propagation). In this case, the small diffusion part of the photorefractive nonlinearity is known to only

cause adiabatic soliton self-bending [29]. A possible way to launch spatial shock waves in biased photorefractives was suggested in Ref. [30]. In this work, a family of stationary shocklike solutions was numerically obtained by solving the beam evolution equation in the so-called Kerr regime. These latter kink states are possible by combining the self-action effects of the drift nonlinearity together with the power exchange (among spatial spectral components) arising from the diffusion component of the space-charge field. In addition, these photorefractive shock-wave solutions can occur in both a self-focusing or defocusing environment and exhibit an oscillatory intensity pattern [30].

In this paper, we describe an alternative avenue through which spatial optical shock waves can be observed in photorefractive crystals. In particular, we demonstrate that the evolution equations describing the interaction between two codirectional beams in unbiased photorefractive media can exhibit a pair of shock-wave solutions. These kinklike solutions are made possible via the two-wave mixing process. These locked kink-antikink shock waves propagate undistorted through the photorefractive crystal even in the absence of any external bias. Our analysis indicates that these kink-type wavefronts move together at an angle that falls outside the initial  $\pm\theta$  sector of propagation. The apparent direction of propagation and the spatial widths of these optical shock-wave beams are directly related to their relative intensity. Pertinent examples are provided to elucidate their behavior.

### II. THEORETICAL MODEL

Let us begin by considering the evolution equations of two codirectional waves propagating inside a photorefractive crystal. These two waves, henceforth referred to as beam  $a$  and beam  $b$ , propagate in the  $xz$  plane at an angle  $-\theta$  and  $+\theta$ , respectively, with respect to the  $z$  axis. For simplicity, let us neglect any variation of these two beams along  $y$  (i.e., they are planar beams) in which case their evolution will

depend only on the spatial variables  $x$  and  $z$ . Moreover, let us also assume that the two optical beams are relatively broad. Hence, diffraction effects can be neglected and the two beams can be treated as quasiplane waves. In the absence of any external bias, these two optical wavefronts can interact with each other via diffusion-induced two-wave mixing as described by the Kukhtarev-Vinetskii transport model [13,14]. When the depth of modulation of the intensity pattern resulting from the interference of these two optical waves is small, the space-charge field equations can be solved perturbatively [13]. In this case, the equations governing the intensity evolution of these two optical beams can be readily obtained from the two-wave mixing formalism, and are given by

$$\frac{\partial I_a}{\partial z} - v \frac{\partial I_a}{\partial x} - \gamma \frac{I_a I_b}{I_d + I_a + I_b} = 0, \quad (1a)$$

$$\frac{\partial I_b}{\partial z} + v \frac{\partial I_b}{\partial x} + \gamma \frac{I_a I_b}{I_d + I_a + I_b} = 0, \quad (1b)$$

where  $I_a$  and  $I_b$  are the intensities of the two beams involved propagating at  $\pm\theta$  with respect to the  $z$  axis. In Eqs. (1) power flows from  $I_b$  to  $I_a$  as a result of nonlinear two-wave mixing amplification. In the linear regime ( $\gamma=0$ ), the solutions of these equations are given by  $I_a = I_{a0}(x + vz)$ ,  $I_b = I_{b0}(x - vz)$ , i.e., the input intensity profiles remain invariant during propagation. The spatial “velocity”  $v$  is related to  $\theta$  through  $v = \tan \theta$ .  $I_d$  is the so-called dark irradiance, which phenomenologically accounts for the thermal generation of electrons in the conduction band [13]. It is important to note that this quantity ( $I_d$ ) can be artificially elevated [25–27], in which case the requirement for a small depth of modulation (i.e.,  $2\sqrt{I_a I_b} \ll I_d + I_a + I_b$ ) can be readily satisfied. The two-wave mixing power-coupling coefficient  $\gamma$  is given by [13]  $\gamma = [k_0 / (n \cos \theta)] [E_p E_d / (E_p + E_d)] \Gamma$ , where  $k_0 = 2\pi/\lambda_0$ ,  $\lambda_0$  is the free-space wavelength, and  $n$  is the crystal’s unperturbed index of refraction.  $E_p$  and  $E_d$ , known as the saturation space-charge and diffusion fields, respectively, are given by  $E_p = eN_A / \epsilon K_g$  and  $E_d = K_B T K_g / e$ . In these expressions,  $K_B$  is Boltzmann’s constant,  $T$  is the absolute temperature,  $N_A$  is the acceptor density,  $\epsilon = \epsilon_0 \epsilon_r$  is the total static permittivity of the crystal,  $e$  is the electronic charge, and  $K_g$  is the absolute value of the so-called grating vector, which is related to the angle  $\theta$  through  $K_g = 2k_0 n \sin \theta$ . Finally, the parameter  $\Gamma$  is given by  $\Gamma = \vec{p}_a \cdot [(n_i^2 n_j^2 \sum_k r_{ijk} s_k) \cdot \vec{p}_b]$ , where the unit vectors  $\vec{p}_a$  and  $\vec{p}_b$  represent the polarization state of the two beams, and the indices  $i, j$ , and  $k$  take the values 1, 2, or 3, which refer to the optical (principal) axes  $\hat{1}$ ,  $\hat{2}$ , and  $\hat{3}$ , respectively.  $n_i$  is the refractive index “seen” by a wave polarized along the  $i$  direction,  $r_{ijk}$  are the electro-optic coefficients, and  $s_k$  represent the projections of the space-charge field unit vector along the principal axes. For simplicity, any loss effects have been omitted in Eqs. (1a) and (1b). In deriving these equations, it was assumed that the donor and acceptor densities were much larger than that of electrons and the tensorial nature of the dielectric permittivity and that of the electron mobility has been neglected.

### III. SPATIAL SHOCK WAVES—RESULTS AND DISCUSSION

In this section we will demonstrate that Eqs. (1) exhibit shock-wave solutions. These represent a pair of kink wave fronts propagating together in the photorefractive crystal. In order to obtain them, let  $I_a(x, z) = I_a(\xi)$  and  $I_b(x, z) = I_b(\xi)$ , where  $\xi$  is a common moving coordinate system given by  $\xi = x - V_e z$ .  $V_e$  is a dimensionless “velocity” associated with the apparent direction of propagation of these two shock beams inside the crystal and can be positive or negative. The angle of propagation  $\varphi$  at which these beams move with respect to  $z$  is given by  $\varphi = \tan^{-1}(V_e)$ . Furthermore, for convenience, let us study the previous evolution equations in a normalized fashion. In order to do so, we scale the intensities of the two optical beams with respect to the dark irradiance  $I_d$ , that is, let  $I_a(\xi) = rI_d X(\xi)$  and  $I_b(\xi) = sI_d Y(\xi)$ , where  $X(\xi)$  and  $Y(\xi)$  are normalized real functions bounded between 0 and 1, and the positive quantities  $r$  and  $s$  stand for the ratio of the maximum intensity of these beams with respect to the dark irradiance. Substituting these latter forms of  $I_a$  and  $I_b$  in Eqs. (1a) and (1b), we obtain

$$\left( \frac{v + V_e}{s} \right) \frac{dX}{d\xi} + \gamma \frac{XY}{1 + rX + sY} = 0, \quad (2a)$$

$$\left( \frac{v - V_e}{r} \right) \frac{dY}{d\xi} + \gamma \frac{XY}{1 + rX + sY} = 0. \quad (2b)$$

From Eqs. (2), it is then straightforward to show that the following quantity remains constant:

$$\left( \frac{v + V_e}{s} \right) X(\xi) - \left( \frac{v - V_e}{r} \right) Y(\xi) = C, \quad (3)$$

where  $C$  is a constant to be determined.

Looking for shock-wave solutions of Eqs. (2), we must use appropriate boundary conditions. In particular, a shock wave is characterized by two infinite tails. One of them reaches asymptotically a constant value (in this normalized case, unity) whereas the other tail is approaching zero. Here, we also assume that the normalized intensity profiles of the two optical beams are “symmetric” with respect to each other. That is, we assume that at the tails where  $Y=1$ ,  $X$  is zero and conversely, at the other end where  $X=1$  then  $Y=0$ . Using the above boundary conditions in Eq. (3), we immediately find that  $C = (v + V_e)/s = -(v - V_e)/r$ , which leads to the result

$$V_e = \frac{s+r}{s-r} v. \quad (4)$$

Using Eqs. (3) and (4) it is then easy to deduce that the two normalized profiles are complementary to each other, i.e.,  $Y(\xi) = 1 - X(\xi)$ . Furthermore, from Eq. (4) it is clear that the special case  $s=r$  is not allowed. Therefore the two optical shock-wave beams must have different maximum intensities. By rewriting Eq. (4) as  $V_e = [1 + 2r/(s-r)]v = -[1 + 2s/(r-s)]v$ , one can readily conclude that the effective transverse velocity parameter is  $V_e > v$  when  $s > r$ , and  $V_e < -v$  when  $r > s$ . Hence the angle  $\varphi$  that defines the direction of propagation of this pair of kink waves lies between

$\theta < \varphi < \pi/2$  when  $s > r$  and  $-\pi/2 < \varphi < -\theta$  when  $s < r$ . This latter result clearly indicates that the apparent direction of propagation of these two beams is always outside the  $\pm\theta$  sector defined by the two initial wavefronts and it is closer to the direction of propagation of the beam with the highest intensity.

By substituting the expression  $Y(\xi) = 1 - X(\xi)$  in Eq. (2a), one obtains

$$\frac{dX}{d\xi} = \frac{\gamma p}{2v} \frac{X(1-X)}{1+pX}, \quad (5)$$

where the dimensionless real parameter  $p$  has been defined as  $p = (r-s)/(1+s)$ . From Eq. (4) it is obvious that  $V_e$  and  $p$  have opposite signs. It is also important to note that, since the case  $s=r$  is not allowed,  $p$  can never be zero. Furthermore, if  $p$  is rewritten in the form  $p = -1 + (1+r)/(1+s)$ , we clearly see that, for every (positive) value of  $s$  and  $r$ ,  $p > -1$ . Since the real function  $X(\xi)$  is bounded between 0 and 1, the quantity  $X(1-X)/(1+pX)$  is never negative. Therefore, if we assume without any loss of generality that the parameter  $v$  and the coupling constant  $\gamma$  are positive, the derivative  $dX/d\xi$  will be positive (and  $dY/d\xi$  negative) when  $p > 0$ , that is, when  $r > s$ , whereas it will be negative ( $dY/d\xi$  positive) when  $s > r$ . This implies that the beam with the highest intensity in this shock-wave pair exhibits everywhere a positive derivative whereas the derivative of the weaker one is negative. This problem could have also been treated with respect to  $Y(\xi)$  by substituting the condition  $Y(\xi) = 1 - X(\xi)$  in Eq. (2b). In this case the  $Y$  differential equation is identical to that of Eq. (5), provided that the parameter  $p$  is replaced with  $p'$  where  $p' = (s-r)/(1+r)$ . These parameters are related through  $1/p + 1/p' = -1$ , or  $p' = -p/(1+p)$ . Thus the normalized intensity function  $X(\xi)$  found for a particular value of  $p$  is symmetrically related to the profile associated with  $-p/(1+p)$ .

Equation (5) can then be integrated to obtain the normalized intensity profile for  $X(\xi)$ , that is

$$\frac{X}{(1-X)^{(1+p)}} = C \exp\left(\frac{\gamma p}{2v} \xi\right), \quad (6)$$

where  $C$  is a constant to be determined by the initial conditions. For presentation purposes it is more convenient to impose a reflection symmetry on this  $X$ - $Y$  shock wave pair. This is accomplished by requiring that at the origin  $X(0) = Y(0) = \frac{1}{2}$ . In this case, Eq. (6) takes the form

$$X/(1-X)^{(1+p)} = 2^p \exp(\gamma p \xi / 2v). \quad (7)$$

In principle, by solving the transcendental Eq. (7), the functional form of  $X(\xi)$  can be determined. Figure 1 shows such a photorefractive shock-wave pair as a function of  $\xi$  when  $\gamma = 40 \text{ cm}^{-1}$ ,  $\theta = 1.02^\circ$  ( $v = 1.78 \times 10^{-2}$ ),  $r = 0.08$ , and  $s = 0.12$ . These values can be easily realized in high-gain photorefractive crystals such as strontium barium niobate (SBN).

Figure 2 on the other hand, depicts the normalized intensity profile of the  $X$  component as a function of  $\xi$  for various values of  $p$ , when the photorefractive gain is  $\gamma = 40 \text{ cm}^{-1}$ , and  $\theta = 1.02^\circ$  ( $v = 1.78 \times 10^{-2}$ ). For simplicity, only profiles associated with positive values of  $p$  are presented in this

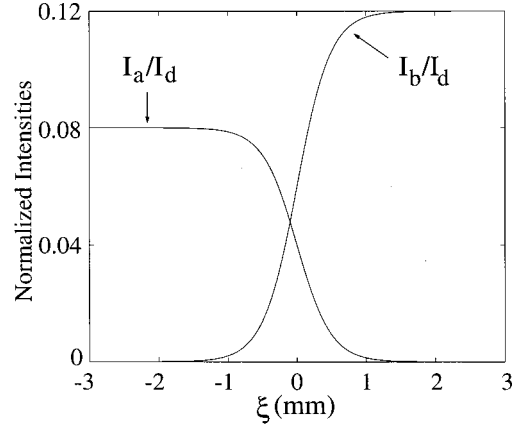


FIG. 1. Normalized intensity profiles of a photorefractive shock-wave pair as a function of  $\xi$  when  $r=0.08$ ,  $s=0.12$ ,  $\gamma=40 \text{ cm}^{-1}$ , and  $\theta=1.02^\circ$ .

figure. As it can be directly observed from Fig. 2, the spatial width of these shock-type profiles varies with the relative intensity ratio  $p$ . We now define the spatial width  $\omega$  of these waves in the following way:  $\omega = |\xi_s - \xi_i|$ , where  $X(\xi_s) = 1 - X_\omega$ ,  $X(\xi_i) = X_\omega$ .  $X_\omega$  in this definition represents a chosen percentage amount with respect to the maximum intensity of this beam. In this case, a straightforward calculation shows that the spatial width of these shock waves is given by

$$\omega = \frac{2v}{\gamma} \frac{(2+p)}{|p|} \ln\left(\frac{1-X_\omega}{X_\omega}\right). \quad (8)$$

From Eq. (8), and by keeping in mind that  $p > -1$ , one can readily show that the spatial width attains its minimum value  $\omega = (2v/\gamma) \ln[(1-X_\omega)/X_\omega]$  at  $p = -1$  and  $p = \infty$ . Conversely, when  $|p|$  is very small, that is, when the relative intensities of both beams are almost the same, the intensity spatial width is given by  $\omega = [4v/(\gamma|p|)] \ln[(1-X_\omega)/X_\omega]$ , i.e., it increases as  $|p| \rightarrow 0$ . It is interesting to note that, in this same regime, the intensity profile  $X(\xi)$  can be analytically obtained from Eq. (7), and it is approximately given by  $X(\xi) = (1/2)[1 + \tanh(\gamma p \xi / 4v)]$ . This solution is identical in nature to that previously found in Ref. [4], within the context of fast and slow Raman shock-wave domains.

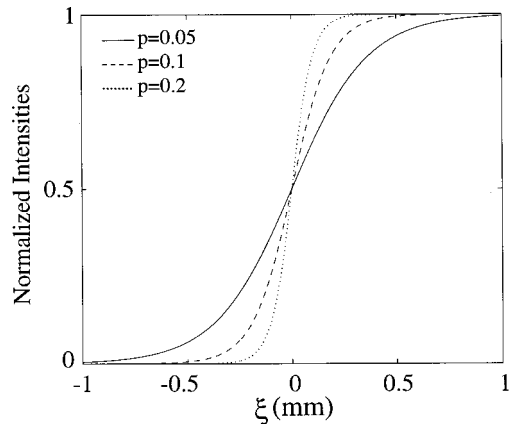


FIG. 2. Normalized intensity profile  $X(\xi)$  of beam  $a$  as a function of  $\xi$  for  $p=0.05, 0.1, 0.2$  when  $\gamma=40 \text{ cm}^{-1}$ , and  $\theta=1.02^\circ$ .

#### IV. EXAMPLES

Let us now illustrate our results by means of relevant examples. Let the photorefractive crystal be of the SBN type, with its optical  $\hat{c}$  axis ( $\hat{3}$ ) directed along the  $x$  direction, that is, let  $\hat{x} \equiv \hat{3}$ . Moreover, let the crystal be oriented in such a way that  $\hat{y} \equiv \hat{2}$  and  $\hat{z} \equiv -\hat{1}$ . Thus, for this particular crystal orientation, the grating vector and the space-charge electric field only have components along the  $\hat{3}$  axis. A straightforward calculation then shows that, in this case [given that SBN is of a symmetry class (4 mm)], the parameter  $\Gamma$  involved in the definition of the coupling constant  $\gamma$  is given by  $\Gamma = n_e^4 r_{33} \cos^2 \theta - n_o^4 r_{13} \sin^2 \theta$ , where  $r_{33}$  and  $r_{13}$  represent, in contracted notation, the electro-optic coefficients  $r_{333}$  and  $r_{113}$ , respectively [13].  $n_e$  is the extraordinary index of refraction whereas  $n_o$  is the ordinary refractive index of this crystal. In deriving this expression, an extraordinary polarization for both beams was also assumed. For SBN,  $r_{33}$  is the dominant electro-optic coefficient and thus, under the previous assumptions, the coupling constant  $\gamma$  is approximately given by  $\gamma \approx (k_0 n_e^4 r_{33} \cos \theta / n) [E_p E_d / (E_p + E_d)]$ , where the unperturbed index of refraction  $n$ , for extraordinary polarized beams, is obtained from  $1/n^2 = \sin^2 \theta / n_o^2 + \cos^2 \theta / n_e^2$  [13]. Let us now assume that the SBN:75 crystal parameters are [31]  $r_{33} = 1022$  pm/V,  $N_A = 4 \times 10^{22}$  m $^{-3}$ ,  $n_e \approx n_o \approx 2.3$ , which means that  $n \approx 2.3$  and  $\varepsilon_r = \varepsilon / \varepsilon_0 = 1000$ , where  $\varepsilon_0$  is the free-space dielectric permittivity. The photorefractive crystal is assumed to be at room temperature and the free-space wavelength of the lightwave employed is taken to be  $\lambda_0 = 0.5$   $\mu$ m. In all cases discussed in this section, the two-wave mixing interaction takes place well within the Bragg regime. In this example  $\theta = 1.4^\circ$ , from where one finds that  $v = 2.44 \times 10^{-2}$  and  $\gamma = 53.2$  cm $^{-1}$ . Furthermore, let the intensity ratios be  $r = 0.08$  and  $s = 0.16$ , in which case  $p = -0.069$ . The transverse velocity of these shocks can be determined from Eq. (4), and  $V_e = 7.32 \times 10^{-2}$ . If we now define the spatial width as the distance between the points where each wave attains 10% and 90% of its peak value ( $X_\omega = 0.1$ ), then for this data one finds from Eq. (8) that  $\omega = 564$   $\mu$ m. For such a broad width, diffraction effects are indeed negligible, a fact consistent with our earlier assumptions. The actual angle  $\varphi$  at which these shock waves propagate with respect to the  $z$  axis is  $4.19^\circ$  (outside the  $\pm 1.4^\circ$  sector). As previously noted, this pair moves more toward the side of beam  $I_b$ , which exhibits the highest intensity ratio. Figure 3 shows the propagation dynamics of these two kink-antikink shock waves as a function of distance. At a distance  $z = 1$  cm, the two locked beams have been laterally displaced by  $x_d = V_e z = 732$   $\mu$ m. Note that for this same distance, each beam alone (in the absence of any two-wave mixing) would have traveled  $x_d = \pm v z = \pm 244$   $\mu$ m, as shown in Fig. 4. In this case, the difference between these displacements is  $488$   $\mu$ m for the  $I_b$  beam and  $976$   $\mu$ m for  $I_a$ . This appreciable shift can be easily detected experimentally. Physically, this process can be understood as follows. As previously noted, power flows from beam  $b$  to beam  $a$  via two-wave mixing. This exchange occurs primarily in the tail region of these two shock-wave beams. In this case, the amplification of beam  $a$  and the depletion of beam  $b$  occur in a self-similar way. As a result of these two beams coalescing,

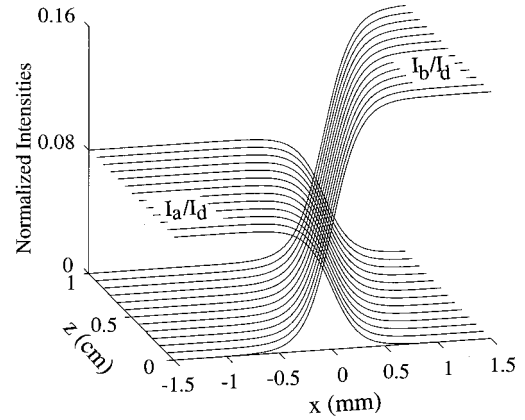


FIG. 3. A shock-wave pair propagating in SBN:75 crystal when  $r = 0.08$ ,  $s = 0.16$ ,  $\gamma = 53.2$  cm $^{-1}$ , and  $\theta = 1.4^\circ$ .

the shock-wave pair attains an apparent transverse velocity, which lies outside the original  $\pm \theta$  range. In this example where  $s > r$ , the two shock waves shift along the positive  $x$  direction, i.e., toward the beam with the highest intensity ( $b$ ). We would like to stress that the tails of these shocks play an important role in this process. In essence they “prepare” the way for this self-similar exchange to occur and the two shocks move at a higher velocity  $V_e$ . For this same reason however, this shock shift can not occur indefinitely. This is because the tail of beam  $a$  (to be amplified) will eventually reach the noise floor of the system after a certain distance. Yet, this process can be observed as long as the differential beam shifts are of the order of the spatial beam widths where the beam power is above the noise level.

The stability of these shock-wave pairs was investigated by means of computer simulations. This was done by numerically solving Eqs. (1). Our simulations show that reasonably small perturbations on any of the two envelopes (or both) do not prevent the simultaneous shifting and locking of the two shock-wave beams. In other words, the shock-wave solution is quite stable and thus should be observable at least within the realistic distances given in our examples. Figure 5 depicts the case where a 10% perturbation was uniformly imposed on the  $X(x)$  component right at the origin (dotted curve). All other parameters are identical to those used in

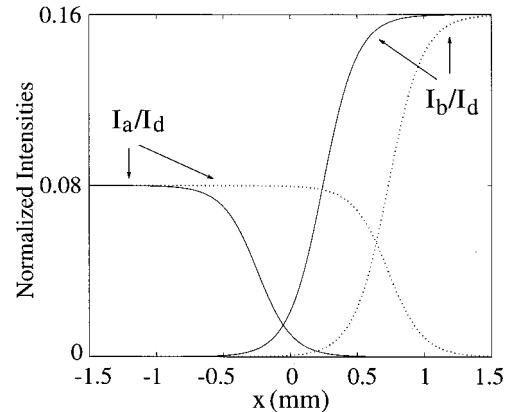


FIG. 4. A shock-wave pair shown after 1 cm of propagation with two-wave mixing (dotted curve) and without two-wave mixing (solid curve). The initial conditions are the same as in Fig. 3.

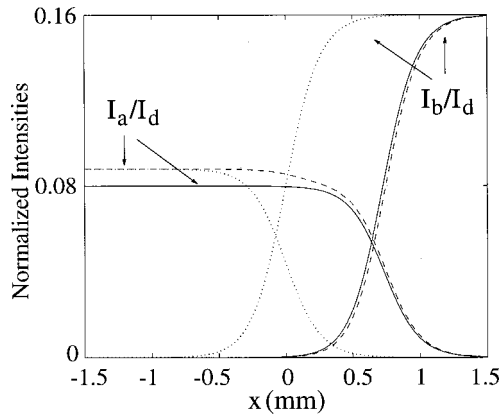


FIG. 5. Stability properties of the photorefractive shock-wave pair shown in Fig. 3. The  $X(x)$  component was uniformly perturbed by 10% whereas  $Y(x)$  remained unchanged. The dotted curve shows the perturbed configuration at the input. Intensity profiles of this shock-wave pair after 1 cm of propagation with this perturbation (dashed curve) and without perturbation (solid curve).

Fig. 3. After 1 cm of propagation, the beams with (dashed curve) or without (solid curve) this perturbation are also shown. It is clear from this figure that the shock-wave pair remains stable and as a matter of fact, it shifts a little faster as compared to the unperturbed case since more power is now involved. In addition, other simulations with localized perturbations on the tails and around the center region have been performed. In all cases, we have found that the wave-locking and shifting mechanism still persists in spite of these perturbations.

Another scenario occurs when the roles of beams  $a$  and  $b$  are reversed, that is, when beam  $a$  has a higher intensity ( $r > s$ ). In order to study this case, let  $r=0.16$ ,  $s=0.08$ , in which case the parameter  $p=0.074$  is positive. The initial angles  $\theta$  are taken here to be  $1.4^\circ$  and thus  $v=2.44 \times 10^{-2}$ . From this data one finds that  $\omega=564 \mu\text{m}$ ,  $V_e=-7.32 \times 10^{-2}$ , and therefore  $\varphi=-4.19^\circ$ . This interaction is shown in Fig. 6 up to a distance of 1 cm. In this example, the two shocks move together toward the negative semiaxis at an angle below that of beam  $a$ . This apparent direction can again be understood keeping in mind that beam  $a$  is amplified at the expense of  $b$ . After 1 cm of propagation, the two locked beams have shifted by a distance  $x_d = V_e z = -732 \mu\text{m}$ . For this same distance, each beam alone (in the absence of any two-wave mixing) would have traveled  $x_d = \pm v z = \pm 244 \mu\text{m}$ .

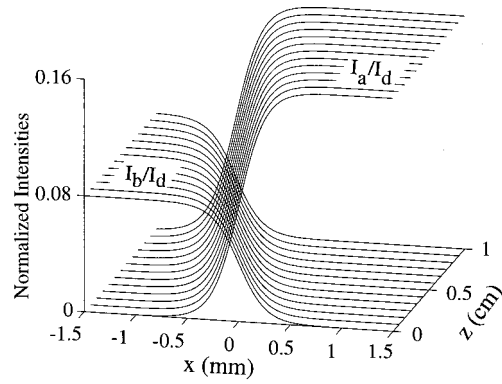


FIG. 6. A shock-wave pair propagating in SBN:75 crystal when  $r=0.16$ ,  $s=0.08$ ,  $\gamma=53.2 \text{ cm}^{-1}$ , and  $\theta=1.4^\circ$ .

Before closing, we would like to emphasize again that there is a marked difference between the spatial shock waves reported here and those suggested in Ref. [30]. First of all, the photorefractive shocks reported in [30] exist through a combination of drift and diffusion nonlinearity and they involve only one component. In contrast, in our work, the wave solution involves a pair of shocks fronts that is possible in unbiased photorefractives (i.e., only diffusion nonlinearity is required). In addition, these locked states must move outside their normal sector of propagation, unlike that of [30], which propagates along the  $z$  axis.

## V. CONCLUSIONS

In conclusion, we demonstrated that the evolution equations describing the interaction between two codirectional beams in photorefractive media can exhibit a pair of shock-wave solutions. These kinklike solutions are made possible via the two-wave mixing process. These locked shock waves propagate undistorted through the photorefractive crystal even in the absence of any external bias. Our analysis indicates that these kink-type wavefronts move together at an angle that falls outside the initial  $\pm\theta$  sector of propagation. The apparent direction of propagation and the spatial widths of these optical shock-wave beams are directly related to their relative intensity.

## ACKNOWLEDGMENTS

This project was financially supported by ARO-MURI, AFOSR, NSF, and ARO.

- [1] M. A. Liberman and A. L. Velikovich, *Physics of Shock Waves in Gases and Plasmas* (Springer-Verlag, Heidelberg, 1986).
- [2] F. V. Shugaev and L. S. Shtemenko, *Propagation and Reflection of Shock Waves* (World Scientific, Singapore, 1998).
- [3] Yu. S. Kivshar, *Phys. Rev. A* **42**, 1757 (1990).
- [4] D. N. Christodoulides, *Opt. Commun.* **86**, 431 (1991).
- [5] G. P. Agrawal and C. Headley III, *Phys. Rev. A* **46**, 1573 (1992).
- [6] Yu. S. Kivshar and B. A. Malomed, *Opt. Lett.* **18**, 485 (1993).
- [7] D. N. Christodoulides and M. I. Carvalho, *Opt. Lett.* **19**, 251 (1994).
- [8] D. Cai, A. R. Bishop, N. Grønbech-Jensen, and B. A. Malomed, *Phys. Rev. Lett.* **78**, 223 (1997).
- [9] D. E. Pelinovsky, Yu. S. Kivshar, and V. V. Afanasjev, *Phys. Rev. E* **54**, 2015 (1996).
- [10] W-S. Kim and H-T. Moon, *Phys. Lett. A* **266**, 364 (2000).
- [11] A. Kobayakov, S. Darmanyan, T. Pertsch, and F. Lederer, *J. Opt. Soc. Am. B* **16**, 1737 (1999).
- [12] Self-steepening shocks can also develop in dispersionless nonlinear systems. In this case however, no kink solutions are possible. Instead, a wave develops a steep front during propagation. See, for example, F. De Martini, C. H. Townes, T. K.

- Gustafson, and P. L. Kelley, *Phys. Rev.* **164**, 312 (1967); D. Anderson and M. Lisak, *Phys. Rev. A* **27**, 1393 (1983).
- [13] P. Yeh, *Introduction to Photorefractive Nonlinear Optics* (Wiley, New York, 1993).
- [14] N. Kukhtarev, V. B. Markov, S. G. Odulov, M. S. Soskin, and V. L. Vinetskii, *Ferroelectrics* **22**, 949 (1979).
- [15] P. Günter and J.-P. Huignard, *Photorefractive Materials and their Applications I*, Topics in Applied Physics Vol. 61 (Springer, Heidelberg, 1998).
- [16] M. P. Petrov, S. I. Stepanov, and A. V. Khomenko, *Photorefractive Crystals in Coherent Optical Systems* (Springer, Heidelberg, 1991), Vol. 59.
- [17] P. Günter, *Phys. Rep.* **93**, 199 (1982), and references therein.
- [18] P. Yeh, *IEEE J. Quantum Electron.* **25**, 484 (1989).
- [19] Y. H. Ya, *Opt. Quantum Electron.* **14**, 547 (1982).
- [20] J.-P. Huignard and A. Marrakchi, *Opt. Commun.* **38**, 249 (1981).
- [21] Ph. Refregier, L. Solymér, H. Rajbenbach, and J.-P. Huignard, *J. Appl. Phys.* **58**, 45 (1985).
- [22] M. Segev, B. Crosignani, A. Yariv, and B. Fischer, *Phys. Rev. Lett.* **68**, 923 (1992).
- [23] B. Crosignani, M. Segev, D. Engin, P. Di Porto, A. Yariv, and G. Salamo, *J. Opt. Soc. Am. B* **10**, 446 (1993).
- [24] G. C. Duree, J. L. Shultz, G. J. Salamo, M. Segev, A. Yariv, B. Crosignani, P. Di Porto, E. J. Sharp, and R. R. Neurgaonkar, *Phys. Rev. Lett.* **71**, 533 (1993).
- [25] M. Segev, G. C. Valley, B. Crosignani, P. Di Porto, and A. Yariv, *Phys. Rev. Lett.* **73**, 3211 (1994).
- [26] D. N. Christodoulides and M. I. Carvalho, *J. Opt. Soc. Am. B* **12**, 1628 (1995).
- [27] M. D. Castillo, P. A. Aguilar, J. J. Sanchez-Mondragon, S. Stepanov, and V. Vysloukh, *Appl. Phys. Lett.* **64**, 408 (1994).
- [28] G. C. Valley, M. Segev, B. Crosignani, A. Yariv, M. M. Fejer, and M. C. Bashaw, *Phys. Rev. A* **50**, R4457 (1994).
- [29] M. I. Carvalho, S. R. Singh, and D. N. Christodoulides, *Opt. Commun.* **120**, 311 (1995).
- [30] V. A. Vysloukh, V. Kutuzov, V. M. Petnikova, and V. V. Shuvalov, *Zh. Eksp. Teor. Fiz.* **111**, 705 (1997) [*JETP* **84**, 388 (1997)].
- [31] R. A. Vazquez, R. R. Neurgaonkar, and M. D. Ewbank, *J. Opt. Soc. Am. B* **9**, 1416 (1992).